Journal of Building Engineering 106 (2025) 112671

Contents lists available at ScienceDirect

Journal of Building Engineering

journal homepage: www.elsevier.com/locate/jobe

A state-of-the-art approach for the direct and indirect measurements of the ultrasonic wave reflection on the fresh cement paste in determining the setting behavior via Fourier transformations

Harry Hermawan [a,*], Fariz Rifqi Zul Fahmi [b]

[a] National Taiwan University of Science and Technology, Department of Civil and Construction Engineering, No. 43, Section 4, Keelung Road, Da'an District, 106 Taipei, Taiwan
[b] UIN Maulana Malik Ibrahim, Department of Mechanical Engineering, Malang, 65144, Indonesia

ARTICLE INFO

Keywords:
Setting time
Ultrasonic wave reflection
Shear wave
Cement paste
Fourier transform

ABSTRACT

The setting and hardening of cement paste were crucial for casting fresh concrete in the field, as they directly impact the timing and cost of framework removal and other operations. The conventional Vicat needle test for setting time had several drawbacks, including being manually operated, time-consuming, irreproducible, and non-continuous. To address these issues, two ultrasonic methods (ultrasonic wave reflection direct (UWRD) and ultrasonic wave indirect (UWRI)) were developed to monitor the stiffening process of cement paste. These methods analyzed waveform signals of longitudinal (P-wave) and shear (S-wave) waves that reflect at material boundaries (UWRD: paste-air interface; UWRI: acrylic-paste interface). The signals were processed using Fast Fourier Transform (FFT) and Short Time Fourier Transform (STFT). Cement pastes with three water-to-cement ratios (0.30, 0.40, 0.50) were tested, and results showed that both methods accurately predicted the final setting time. The UWRD method determined the final setting time over 95 % accuracy by detecting the first reflected P-wave, although it could not measure the initial setting time due to noise interference. The UWRI method identified the final setting time based on the lowest amplitude point of the S-wave reflection with a minor deviation of less than 6 % from the traditional measurement. The proposed UWRD and UWRI were effective, reliable alternatives to conventional methods for monitoring the setting behavior of cement paste. By providing automated, continuous, and reproducible measurements, these techniques have the potential to improve quality control in concrete construction and optimize scheduling in field applications.

1. Introduction

Monitoring the initial and final setting times of cement paste is notable to ensuring that concrete remains workable for a sufficient time. Understanding these appropriate times allows for the optimization of formwork removal, the safe application of post-tensioning forces, efficient production of precast elements and the other application of loads in the field, ultimately enhancing workforce

* Corresponding author.
E-mail address: harry.hermawan@mail.ntust.edu.tw (H. Hermawan).

https://doi.org/10.1016/j.jobe.2025.112671
Received 1 January 2025; Received in revised form 6 April 2025; Accepted 13 April 2025
Available online 14 April 2025

Nomenclature

A_i	amplitude of incident wave
$A_{reflection}$	amplitude of reflected wave
$A_{transmission}$	amplitude of transmitted wave
$D_{t_c - t_f}$	percentage difference between t_c and t_f
$D_{t_s - t_f}$	percentage difference between t_s and t_f
$F_1^{acrylic-air}$	magnitude of FFT at acrylic–air interface
$F_1^{acrylic-paste}$	magnitude of FFT at acrylic–paste interface
ρ	density of material
$r(f)$	normalized FFT peak amplitude
R	coefficient of reflection
t_c	time at the critical point where the FFT curve initially changes its slope
t_f	standardized final setting time of cement paste
t_i	standardized initial setting time of cement paste
t_s	time at the specific point where the FFT curve reaches the minimum point
T	coefficient of transmission
V	ultrasound velocity
w/c	water-to-cement ratio
Z	acoustic impedance
Z_1	acoustic impedance of the first media
Z_2	acoustic impedance of the second media

efficiency. The stiffening and hardening of cement paste primarily result from the hydration reaction between cement particles and water. During this process, there is a progressive transition in the cement paste where it transforms from a liquid to a solid state [1]. As cement reacts with water, the continuous formation and interaction of hydration products [2] cause the cement paste to set. The term of "setting" refers the gradual stiffening of the paste, while the "hardening" corresponds to the development of mechanical properties of the paste over time [3].

Penetration needle methods are commonly used to determine the setting times of Portland cement paste. Conventionally, the two standard tests for this measurement are the Vicat needle test and the Gillmore needle test in accordance with ASTM C191 [4] and ASTM C266 [5], respectively. Both methods follow a similar approach and are restricted to laboratory testing. The fundamental of Vicat and Gillmore tests is based on the penetration depth of a needle. However, for the same specimen, different methods will obtain different setting time values. The definitions of initial and final setting times are somewhat subjective, as the measured values depend on the sensitivity of the testing method. While Vicat and Gillmore tests are simple and cost-effective, they are laborious, manually operated, time-consuming and susceptible to errors–especially when applied to rapid-setting mixtures where interpolation may introduce inaccuracies. To overcome these limitations, researchers have explored non-destructive alternatives, such as ultrasonic testing, for a more reliable and continuous assessment of the setting behavior of cement paste.

Ultrasonic testing has gained significant attention for evaluating the properties of cement paste during hydration. Unlike penetration-based methods, ultrasonic techniques analyze the wave propagation through the paste, providing real-time insights into its evolving structure. The velocity and attenuation of ultrasonic waves are generally influenced by hydration-related factors such as density and porosity [6]. A higher water-to-cement (w/c) ratio results in slower wave propagation due to increased porosity and reduced stiffness [7], whereas a lower w/c ratio facilitates faster wave transmission. The hydration process and microstructure development also impact ultrasonic behavior. In the early stages, when the paste is still fluid, shear waves are unable to propagate effectively, while compressional waves can still travel [8]. As hydration products like calcium silicate hydrate (C-S-H) and calcium hydroxide (CH) form, the paste stiffens, improving wave transmission [9]. Viscosity and rheology influence the coupling efficiency between the transducer and the material, directly affecting signal quality [10]. Additionally, temperature and moisture content alter wave velocity [11], as rising temperature accelerates hydration, leading to rapid changes in stiffness. Finally, the presence of admixtures and supplementary cementitious materials (SCMs), such as fly ash or silica fume, modifies pore structure and hydration kinetics, further influencing ultrasonic wave speed and attenuation [12]. Understanding these factors is essential for accurately interpreting ultrasonic test results in cement-based materials.

A few quantitative setting time measurements on cement paste are relatively difficult because the cement-based material is classified as a heterogeneous material that exhibits a high attenuation [13]. This attenuation leads to the disturbance of signal in the form of noise and as a result, the transition time of the fresh paste is hard to be distinguished especially before the setting stage [14,15]. In recent years, non-destructive ultrasonic measurement has been used widely and it turns out to be an effective and promising method for monitoring the stiffening process of cement-based composite. Ultrasonic pulse velocity (UPV) applications estimate the setting time of cement paste by continuously measuring the speed of ultrasonic waves passing through the material as it hydrates and hardens. The setting process of cement paste involves complex chemical reactions [16], primarily the hydration of clinker compounds, which lead to the formation of a rigid structure. Initially, in the fresh state, the paste has a low stiffness and high porosity, causing ultrasonic waves to

travel slowly with significant attenuation. As the hydration process progresses, solid phases begin to form, increasing the rigidity of the paste, consequently increasing ultrasonic velocity over time. By analyzing the velocity-time curve, characteristic points corresponding to the initial setting time (when the paste begins to lose plasticity) and the final setting time (when it gains sufficient rigidity) can be identified. These setting times are determined based on the rapid increase in wave velocity due to the formation of a continuous solid skeleton within the paste [17].

On the other hand, the ultrasonic reflection test can also be considered using a buffer material as the medium to monitor the alteration of wave reflection from the boundary of buffer material and paste. In this way, it is possible to evaluate the setting of cement-based materials starting from a liquid state until a solid state. This aforementioned method can be called as "indirect method" since the waves are not generated directly to the paste, but the waves are inspected via a buffer material. For instance, Öztürk et al. [18,19] performed the experimental work using acrylic glass as a buffer material and L-wave transducer with the central frequency of 200 kHz. Their result showed that the initial setting time was determined using the numerical derivative of wave reflection factor (WRF), known as the different quotient (DQ) and the zero-crossing of the DQ corresponded to the final setting time. Chung et al. [20,21] monitored the longitudinal and shear reflection responses from the boundary of high impact polystyrene (HIPS) material and cement paste. The final setting time was measured from the longitudinal wave (P-wave) ultrasonic wave reflection (UWR) curves, specifically at the onset of the third stage of P-wave reflection behavior, where partial debonding occurred due to water under pressure at the paste-buffer interface. Trtnik et al. [22,23] reported that the change of shear wave reflection coefficient was sensitive to the formation of internal structure in the pastes. Moreover, Yim et al. [24] explained the importance of the frequency dependence to monitor the mechanical impedance of cement-based material. The compressive strength of concrete at the early ages can be predicted based on the reflection loss from the interface of steel plate and concrete non-destructively [25]. The reflection loss had a good correlation with early age compressive strength with the coefficient of determination above 0.97, as suggested by Ref. [26]. Furthermore, the relationship between reflection loss and compressive strength was found to be affected by the curing temperature [27]. The reflection wave response from the interface of acrylic and mortar was conducted by Subramaniam et al. [28] and the results showed that the amplitude of reflected waves decreased gradually until reaching a minimum, after which it began to increase as the mortar stiffened at later ages. Suraneni et al. [29] reported that the results of ultrasonic wave reflection coefficient were reproducible and had a potential in determining the setting time. Moreover, Voigt et al. [30] found that the reflection coefficient closely correlated with the degree of hydration and varied with different w/c ratios. When the ultrasonic wave reflection was applied to concrete, the aggregates and the interfacial transition zone (ITZ) played a crucial role in influencing impedance properties [31]. Nam et al. [32] also confirmed that the ultrasound transmission was affected by the porosity and density of aggregates.

The ultrasonic wave reflection indirect (UWRI) method is a commonly used technique that has been widely employed in past research [18–24,26–30], utilizing a buffer material to facilitate wave reflection. Although it can be used to observe the setting process, the elastic waves are not directly introduced into the paste. Instead, the waves are reflected through the buffer material, leading to the reflection loss [33] due to paste hardening. When the impedance of the tested material exceeds that of the buffer, a sudden change in reflection behavior occurs [34]. However, the lack of relevant standards for selecting buffer materials makes it challenging to monitor the setting behavior when different buffers are used. This limitation presents a challenge, as the indirect transmission of waves affects measurement accuracy.

Consequently, a new approach was developed using the ultrasonic wave reflection direct (UWRD) method. In this method, an ultra-thin acrylic was used as a medium, allowing waves to be introduced directly into the paste. The main objective of this research was to develop an innovative, simple, efficient and non-destructive technique using both UWRD and UWRI methods to determine the setting time of Portland cement paste by analyzing the wave reflection responses at the boundary condition.

2. Wave propagation theory

Ultrasound is defined as sound wave in the form of elastic waves with a frequency greater than 20 kHz, exceeding the maximum detection limit of the human ear. Ultrasound is not limited to sound waves traveling through gases and liquid but also includes more complex elastic waves in solids. Sound propagation in solids plays a prominent role in ultrasonic applications and it is more complex than the propagation in liquids due to the material's ability to resist changes in both volume and shape [35].

In general, the propagation of ultrasonic waves is influenced by boundary surfaces. When an incident wave encounters the interface between two media, it can be either transmitted, reflected or refracted, with changes in both amplitude and speed. Wave propagation occurs as materials respond to sound pressure, which induces molecular vibrations that travel through the solid. Because molecules or atoms in a solid are elastically bound to one another, an excess pressure leads to wave propagation throughout the material [36]. The material property known as acoustic impedance (Z) is an important parameter when an elastic wave is introduced into a material. It is defined as the ratio of sound pressure to particle velocity at a given point in the medium and depends on both the material's density (ρ) and wave velocity (V). Acoustic impedance is mathematically expressed as:

$$Z = \rho V \tag{1}$$

where Z is acoustic impedance (Rayls), ρ is density of material (kg/m^3), and V is ultrasound velocity (m/s). The role of acoustic impedance is necessary in determining the acoustic transmission and reflection at the boundary of two materials having different acoustic impedances [18,21,28], also in designing ultrasonic transducer and assessing the absorption of sound in medium. When an incident wave penetrates into two media, the amplitude of reflected and transmitted waves can be computed using following equations:

$$A_{reflection} = A_i \frac{(Z_2 - Z_1)}{(Z_2 + Z_1)} \tag{2}$$

$$A_{transmission} = A_i \frac{2Z_2}{(Z_2 + Z_1)} \tag{3}$$

$$R = \frac{A_{reflection}}{A_i} = \frac{(Z_2 - Z_1)}{(Z_2 + Z_1)} \tag{4}$$

$$T = \frac{A_{transmission}}{A_i} = \frac{2Z_2}{(Z_2 + Z_1)} \tag{5}$$

where $A_{reflection}$ is amplitude of reflected wave (volt), $A_{transmission}$ is amplitude of transmitted wave (volt), A_i is amplitude of incident wave (volt), R is coefficient of reflection, T is coefficient of transmission, Z_1 is acoustic impedance of first media (Rayl) and Z_2 is acoustic impedance of second media (Rayl). Both the reflection coefficient and transmission coefficient are strongly influenced by the acoustic impedance of material. Typically, when an incident wave encounters the boundary between two media, it exhibits three major types of reflection behaviors. The first case is when impedance of first material is much lower than the impedance of second material ($Z_1 \ll Z_2$). According to the principle, $A_{reflection}$ and $A_{transmission}$ approach A_i and $2A_i$, respectively. It implies that there are no phase changes as the reflection coefficient is equal to one. In the second case, when impedance of first material is much higher than the impedance of second material ($Z_1 \gg Z_2$), then $A_{reflection}$ and $A_{transmission}$ approach $-A_i$ and 0, respectively. It indicates that the transmission will not occur as the transmission coefficient equals to zero. In the third case, when the impedances of both first and second materials are equal ($Z_1 = Z_2$), $A_{reflection}$ is equal to zero while $A_{transmission}$ is equal to one. It marks that the reflection does not occur as R equal to zero and the incident waves are fully transmitted into the second media.

3. Materials and methods

3.1. Materials

The commercial Type I ordinary Portland cement (OPC) in accordance to ASTM C150 [37] was used as the main binder to produce cement pastes. The chemical and physical properties of OPC are presented in Table 1. Cement pastes with three water-to-cement ratios (w/c) were made at 0.30, 0.40 and 0.50 (hereinafter, the pastes were labelled as OPC 0.3, OPC 0.4 and OPC 0.5, respectively).

3.2. Ultrasonic wave reflection direct (UWRD) method

In this study, a newly proposed technique, the ultrasonic wave reflection direct (UWRD) method, was developed to examine the setting process of cement paste using ultrasound. The key advantage of the UWRD method over the conventional UWRI method was that the signal transmitted and reflected within the paste itself, eliminating the need for a buffer material. Prior studies likely did not adopt the UWRD method due to several challenges. First, fresh cement paste was highly attenuative, causing weak reflections and considerable noise interference. Second, transmission-based methods like UPV were preferred for their clearer and robust measurements. Third, the paste-air interface lacked strong acoustic contrast, making reflections harder to detect. In comparison, methods like UWRI, which rely on a buffer material for wave reflection, introduce additional challenges such as a partial debonding (or loss of physical contact) between the paste and buffer due to autogenous shrinkage [21], potentially distorting the signals.

The schematic testing setup of UWRD measurement is shown in Fig. 1a. A broadband longitudinal wave (P-wave) transducer type Olympus A114S with a central frequency of 1.0 MHz was used. This transducer frequency was selected based on a preliminary study by authors, which found that higher frequencies (e.g., 2.25 MHz) resulted in greater material attenuation in heterogeneous material like cement paste, leading to signal loss. By using a lower frequency transducer (e.g., 1.0 MHz), a clearer signal was obtained, allowing for better representation and effective monitoring of reflection changes over time. An ultra-thin acrylic sheet (0.5 mm thick) was used to attach the transducer beneath the mould. Acrylic was chosen due to its relatively low acoustic impedance, and because the sheet was extremely thin, its influence on wave propagation can be neglected. As a result, the reflection was considered to occur directly at the cement paste-air interface. The paste mould, acting as a standard container for setting time measurement in accordance with ASTM C191 [4], was glued on the top surface of acrylic sheet. The transducer was coupled on the bottom surface of acrylic sheet with the ultrasonic couplant produced by SONOTECH®. Based on the preliminary study, P-wave was found to be more sensitive and suitable for the UWRD method compared to S-wave, as the S-wave signal remained in the noise regime throughout the entire testing period. As a matter of fact, the shear wave cannot travel through liquid because it requires shear stiffness. In the early setting stage, cement paste

Table 1
Chemical and physical properties of ordinary Portland cement (OPC).

Chemical properties								Physical properties	
Comp.	SiO_2	Al_2O_3	Fe_2O_3	CaO	MgO	SO_3	L.O.I	*Specific gravity*	*Blaine fineness* (cm^2/g)
wt.%	20.42	4.95	3.09	61.96	3.29	2.40	1.75	3.15	3450

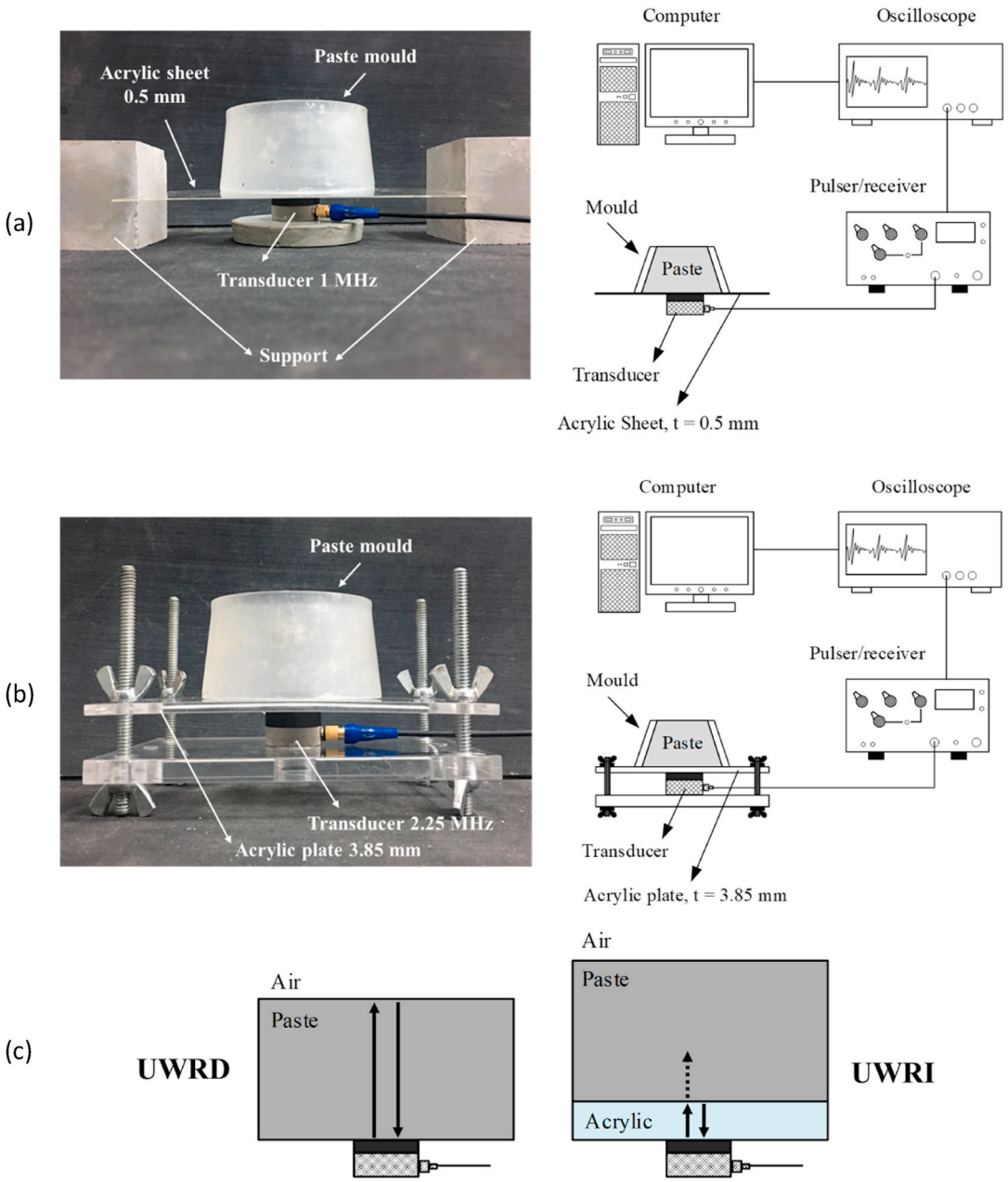

Fig. 1. Testing setup for (a) the ultrasonic wave reflection direct method (UWRD) and (b) the ultrasonic wave reflection indirect method (UWRI); (c) schematic representation of the wave reflection phenomenon in UWRD and UWRI methods.

behaves like a viscous fluid with low stiffness, meaning S-wave cannot effectively propagate, making it unsuitable for early-age monitoring. The S-wave travels slower than the P-wave, resulting in weaker and less distinct signal detection in ultrasonic measurement, particularly for heterogeneous materials like cement paste. On the other hand, P-wave is commonly used to assess the properties of cement-based materials due to its sensitivity to material composition, porosity and microstructural changes. Cement paste, particularly in its early stages, exhibits high porosity which significantly affects P-wave propagation. In contrast with S-wave, P-wave travels faster in solid, dense material and can also propagate through water or liquid. As the setting of cement paste progresses from a liquid to a solid state, more reflection energy is expected via P-wave, potentially leading to a rise in reflection amplitude. In addition, the P-wave reflection method did not disturb the sample, making it ideal for continuous monitoring. Therefore, the P-wave measurement was employed in this study.

3.3. Ultrasonic wave reflection indirect (UWRI) method

The indirect method has been regularly used in past research, utilizing a buffer material (e.g., steel, acrylic, HIPS) as a medium. This method relied on monitoring the reflection changes at the buffer-paste boundary, as the waves did not directly travel to the paste. Fig. 1b shows the schematic testing setup of UWRI measurement. Unlike the UWRD method, a single broadband shear wave transducer (Panametric V154) with a center frequency of 2.25 MHz was used in this method. Unlike the UWRD method, the UWRI method requires a high-frequency transducer because the signal is reflected in a homogeneous material (i.e., acrylic as a buffer material). In this case, higher frequencies enhance wave reflection while reducing material attenuation. An acrylic plate (3.85 mm thick) was used as a buffer material to direct the wave from the transducer to the paste through reflection. The acoustic impedance of acrylic plate was previously measured at 3.30 MRayls. Acrylic was chosen as the buffer material due to its low acoustic impedance and good sensitivity to early changes, enabling the early-age measurement for the cement pastes. The paste mould, compliant with ASTM C191 [4], was attached to the top surface of the acrylic plate, while the transducer was coupled to the bottom surface using an ultrasonic couplant produced by SONOTECH®. Based on our preliminary study, both P-wave and S-wave were applicable in this UWRI method. In fact, the P-wave was generally more robust because compressional waves were faster than shear waves in solid. Nevertheless, the application of P-wave in understanding the stiffening behavior of cement paste has been frequently demonstrated in past studies [18–23]. Thus, it was decided to proceed with the S-wave for this investigation.

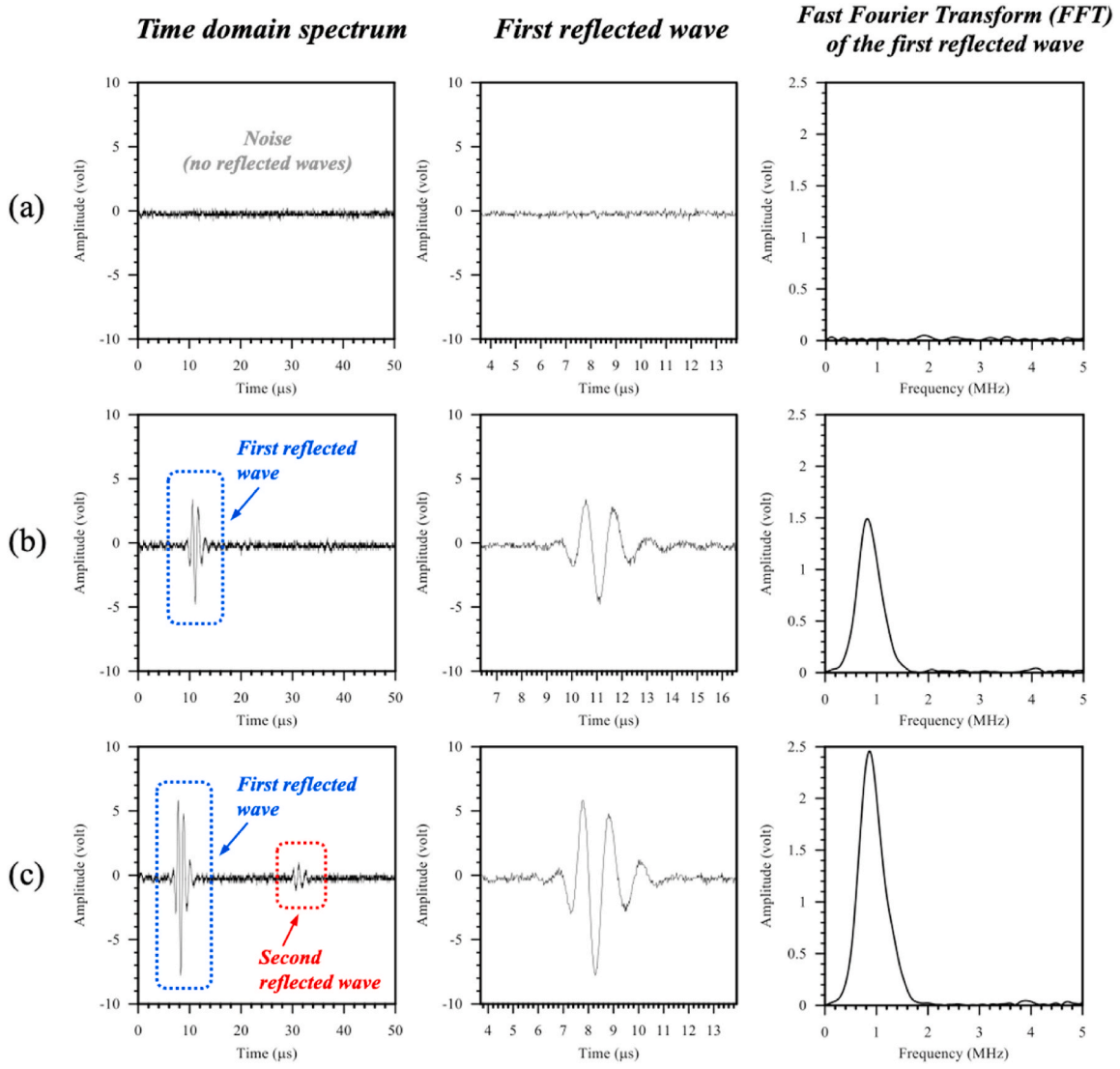

Fig. 2. Transformation of time domain signal into frequency domain signal via FFT on the first reflected wave at (a) 15 min, (b) 600 min, and (c) 1200 min.

3.4. Penetration needle test

The traditional Vicat needle testing was conducted to determine the standardized setting time values in accordance with ASTM C191 [4]. The initial setting time was recorded when the steel needle penetrated 25 mm into the cement paste, while the final setting time was defined as the point when the needle could no longer penetrate into the paste.

3.5. Isothermal calorimetry test

The early hydration mechanism of the cement paste, in relation to the setting behavior, was investigated via an isothermal calorimetry test. The 50-g paste samples with varying *w/c* ratios were tested using the I-Cal 4000 HPC (High Precision Calorimeter) at 25 °C, ensuring the same temperature condition as the ultrasonic testing for a fair comparison. This test provided heat flow curves corresponding to the hydration and setting process.

3.6. Testing procedure

The schematic of the ultrasonic apparatus testing setup is presented in Fig. 1a and b. The transducer was connected to the pulser/receiver type Panametrics 5077 PR via a BNC cable, which was then linked to a digital oscilloscope. The pulser/receiver was used to generate a single 300 V peak square pulse and to receive the reflected waves. The sampling rates were set at 50 MS/s for the direct method and 100 MS/s for the indirect method. The captured waveform signals were recorded using NI LabVIEW program.

After setting up the apparatus, the cement paste was prepared in accordance with ASTM C305 [38]. First, the mixing water was added to the bowl, followed by the cement, with a 30-s waiting period to allow for the water absorption. The mixing began at a slow speed (140 ± 5 r/min) for 30 s, after which the mixer was stopped for 15 s. During this pause, the bottom of the bowl was scrapped to ensure thorough mixing of the cement powder. The mixing then resumed at a medium speed (285 ± 10 r/min) for 60 s. Finally, the cement paste was poured into the mould for testing.

The ultrasonic measurement was started immediately after the mould was completely filled with cement paste. The entire tests were performed inside a controlled chamber at a room temperature of 25 ± 2 °C and a relative humidity of 50 ± 5 %. Ultrasonic raw data were recorded automatically at 15-min intervals until the final testing time of 1200 min (or 20 h). The waveform signals were initially obtained in the time domain signal and later analyzed by applying a Fast Fourier Transform (FFT) to convert them into the frequency domain. The FFT peak amplitudes were extracted and used as the primary basis analysis for determining the setting time of the paste. Additionally, the Short-Time Fourier Transform (STFT) was performed to visualize the time-frequency distribution and to track amplitude development. The aforementioned signal processing was carried out using Visual Signal software (AnCAD Inc., Taiwan).

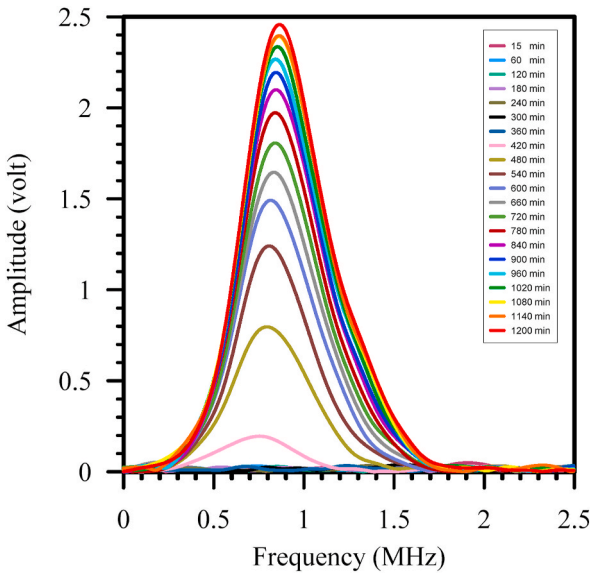

Fig. 3. Evolution of FFT based on the P-wave UWRI measurement (note: OPC 0.3 paste was taken as an example).

4. Experimental results

4.1. Analysis of ultrasonic wave reflection direct method (UWRD) responses

A typical reflected wave in the time domain spectrum and the corresponding FFT result of the first reflected wave are shown in Fig. 2, for example, at 15 min, 600 min and 1200 min for OPC 0.3 paste. At 15 min, since the paste was still in its liquid phase, no significant reflection was observed, resulting in noise. In this case, the transmitted wave did not bounce back to the transducer. Although longitudinal waves can propagate through both solid and liquid, at this early stage, the paste was a suspension consisting of cement and water. The wave did not generate any reflections, indicating that the energy was still too low for reflection. As time progressed, the hydration occurred leading to paste stiffening and a denser microstructure. According to Fig. 2, the first reflected wave appeared later and gradually shifted to the left over time. For instance, at 600 min, the first reflected wave appeared within the 8–16 μs range, and at 1200 min, it shifted to the 5–12 μs range. This shift suggested an increase in wave as hydration progressed. Additionally, the amplitude of the reflected wave increased over time, indicating that stronger reflection energy was penetrating the material.

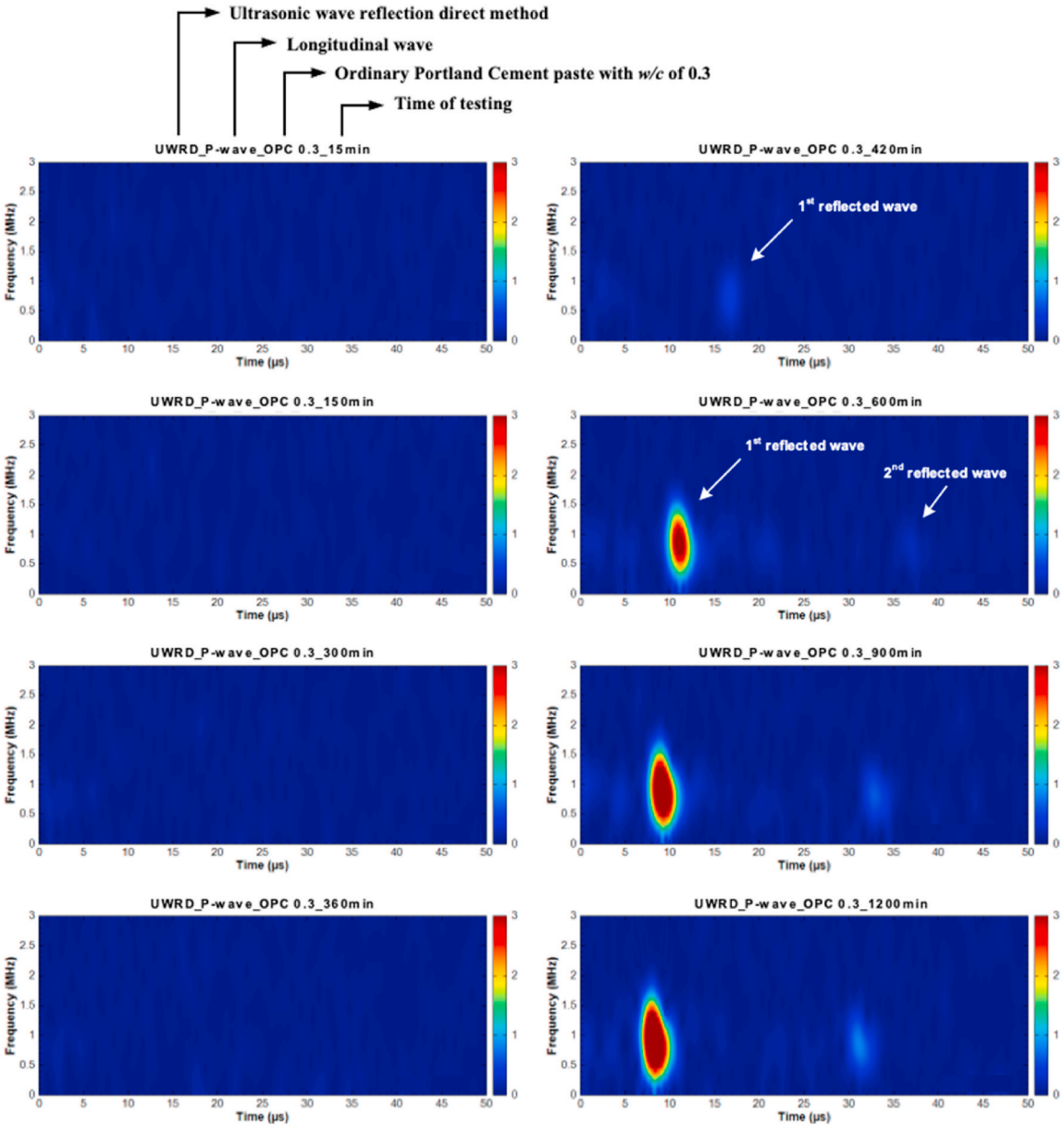

Fig. 4. Development of STFT waveform between 15 and 1200 min using the P-wave reflection at the interface of paste–air (UWRD method) (note: OPC 0.3 paste was taken as an example).

Similar behavior was observed in pastes with different *w/c*.

Fig. 2 illustrates the transformation of the first reflected wave from the time domain to the frequency domain via FFT. At the early stage (15 min), the FFT result showed low signal amplitudes and the peak amplitude was not clearly visible due to noise. The FFT response appeared as a jagged waveform, making the FFT curve unstable. However, at later times, the first reflected waves became more distinct. For instance, at 600 min, the first reflected wave was transformed using FFT, revealing a peak amplitude of approximately 1.5 V at a frequency of 0.8 MHz. The FFT peak amplitude increased over time due to the stiffening process of the cement paste. A typical evolution of FFT over time is depicted in Fig. 3. Moreover, the time domain signal was analyzed using STFT to monitor its evolution in the time-frequency domain, as shown in Fig. 4. At 15 min, the spectrum appeared in blue color representing the noise spectrum. However, after a certain time, a sudden appearance of reflection energy was observed. As time progressed, this reflection energy gradually increased. With an input signal centered at 1.0 MHz, the main frequency components were distributed between 0.5 MHz and 1.5 MHz. Notably, the reflection energy shifted leftward over time, indicating changes in the elastic properties of the cement paste as it continued to hydrate and stiffen.

In the frequency domain, FFT peak amplitudes were recorded, and the relationship between testing time and FFT peak amplitude was established, as shown in Fig. 5. When the signal was predominantly noise, the peak amplitudes remained stable at low values (ranging between 0.03 and 0.05 V), forming a steady baseline from the start of the test until a specific point. This phenomenon is associated with the early formation of solid volume fraction and the spacing of cement particles with the percolated water. The chemical composition of the cement and its mixing ratio with water determines the ionic concentration in the cement suspension, and it can be increased with cement particle dissolution by the hydration process [39]. Simultaneously, initial hydration products begin to form, and the combined influence of these factors is captured in ultrasonic measurements. However, at this stage, the quantity of hydration products remains minimal, preventing the reflected wave from traveling back to the transducer. When the paste stays in the liquid phase, signal attenuation remains very high and it carries minimum signal intensity while passing through the capillary spaces [40]. Beyond this time, the peak amplitude increased progressively until reaching a certain level. This critical point, which denoted as t_c, marked as the moment when the FFT curve first changed its slope. It indicated that the cement paste has fully transitioned from a liquid or semi-solid state into a solid structure. Particularly, this point corresponded to the final setting time of the paste, marking the loss of plasticity as the paste transformed into a solid state. This transition aligned with the appearance of the first reflected wave in the time domain waveform. Once the paste fully solidified, wave propagation changed significantly. The wave was able to reflect off the paste-air interface and return to the transducer, making the reflected waves distinctly observed. The measurable stiffening of the paste, along with associated physical changes, occurred after hydration reaction reached a critical stage and generated a sufficient quantity of hydration products [41]. The percolated solid particles have a contact strength together that contribute to the microstructure development [39], marking the start of the reflection. Yim et al. [39] identified ettringite, monocarboaluminate and C-S-H as the primary reaction products of cement hydration after the final setting time (~9 h). Beyond this stage, more ettringite continues to develop as the remaining gypsum is depleted through the hydration and reacts with aluminate [1]. With time, other hydrates assemble and start filling up the void spaces [40], contributing to structural complexity and further affecting the propagation paths of stress waves [39]. The reproducibility of the UWRD results is demonstrated in Fig. 6, which presents three repeated tests using OPC 0.3 pastes. The UWRD method used in this study showed a good reproducibility, as the critical point t_c appeared at the identical time in all trials.

The results for cement pastes with varying water content are presented in Fig. 7. The critical points t_c were measured at 420, 525, and 720 min for OPC pastes with *w/c* of 0.3, 0.4, and 0.5, respectively. Notably, the point t_c appeared earlier in the OPC 0.3 paste compared to the other pastes, indicating that a lower water content accelerates setting. A higher water content delayed the

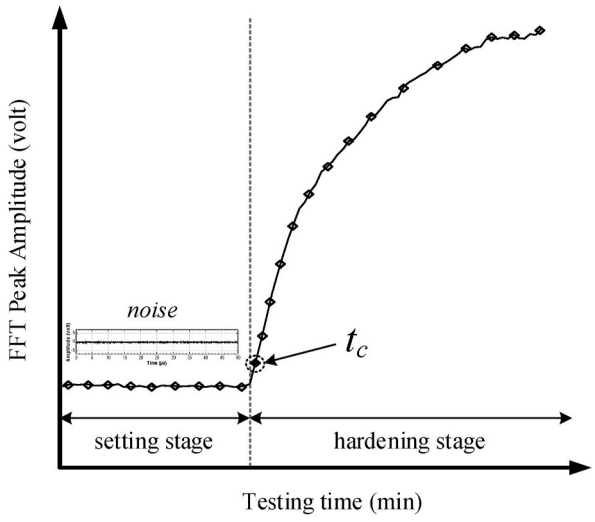

Fig. 5. A typical development of ultrasonic P-wave reflection response in cement paste via UWRD method.

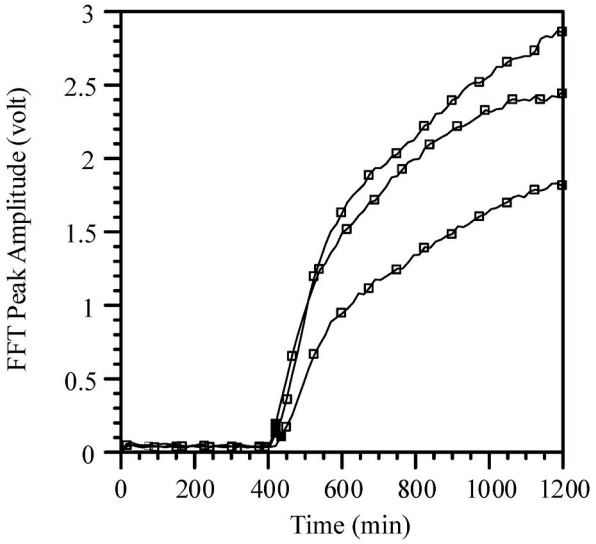

Fig. 6. Reproducibility of UWRD results with triplicates of OPC 0.3 pastes (note: points t_c were marked as filled square bullet).

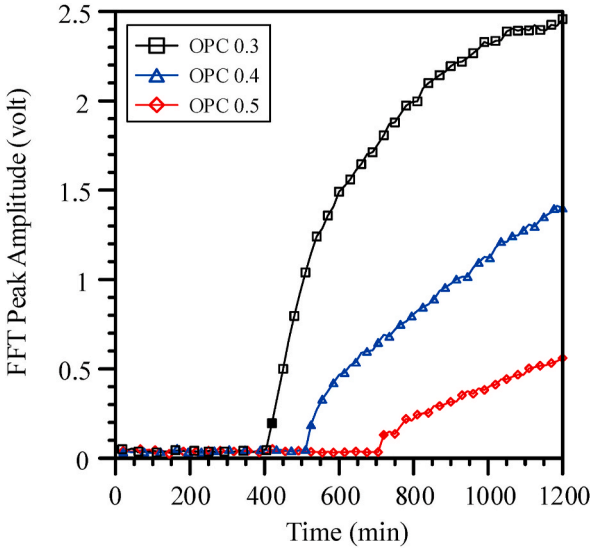

Fig. 7. Development of FFT peak amplitude in function of time on cement pastes with various *w/c* ratios.

development of FFT results, suggesting that the signal was more strongly induced and reflected in pastes with a denser microstructure. At the final testing time, the FFT peak amplitudes were recorded at 2.47, 1.40, and 0.56 V for OPC pastes with *w/c* of 0.3, 0.4, and 0.5, respectively. The strength of signal transmission and the peak frequency highlighted the solidification process in the paste, a

Table 2
Setting time values obtained from the Vicat needle test and UWRD method measurements.

Cement paste	Vicat needle testing		UWRD method (P-wave)		UWRI method (S-wave)	
	t_i (min)	t_f (min)	t_c (min)	Dt_c-t_f (%)	t_s (min)	Dt_s-t_f (%)
OPC 0.3	346	402	420	4.4	405	0.7
OPC 0.4	453	524	525	0.2	555	5.7
OPC 0.5	621	706	720	2.0	705	0.1

Note: t_i, t_f: standardized initial and final setting time by Vicat needle testing, respectively; t_c: time at the critical point where the FFT curve initially changes its slope; t_s: time at the specific point where the FFT curve reaches the minimum point; Dt_c-t_f: the percentage difference between t_c and t_f; Dt_s-t_f: the percentage difference between t_s and t_f.

phenomenon confirmed by autogenous strain tests [42]. Additionally, the reflected signals in OPC 0.3 paste produced higher amplitude compared to pastes with higher *w/c*, indicating greater densification of the internal structure. The progressive increase in FFT amplitudes with hydration further suggested a significant rise in the acoustic impedance of the paste over time.

To validate the ultrasonic measurement results, the setting times of all cement pastes, determined using the Vicat needle test and the UWRD method, are summarized in Table 2. For the OPC 0.3 paste, the standardized initial and final setting times of cement paste were 346 and 402 min, respectively. The final setting time measured using the UWRD method appeared 18 min later than that obtained from the Vicat needle test. Similar trends were observed for the other pastes. For the OPC 0.4 paste, the critical point t_c detected by the UWRD method coincided closely with the final set time of 524 min. In contrast, for the OPC 0.5 paste, the t_c was recorded at 720 min, whereas the Vicat needle test measured the final setting time at 706 min. As shown in Table 2, the t_c from the UWRD method closely matched the t_f from the Vicat needle test. Conclusively, the UWRD method was able to detect the final setting time with a minor deviation of less than 5 % compared to the traditional setting time measurement, demonstrating its accuracy and reliability as an alternative measurement technique.

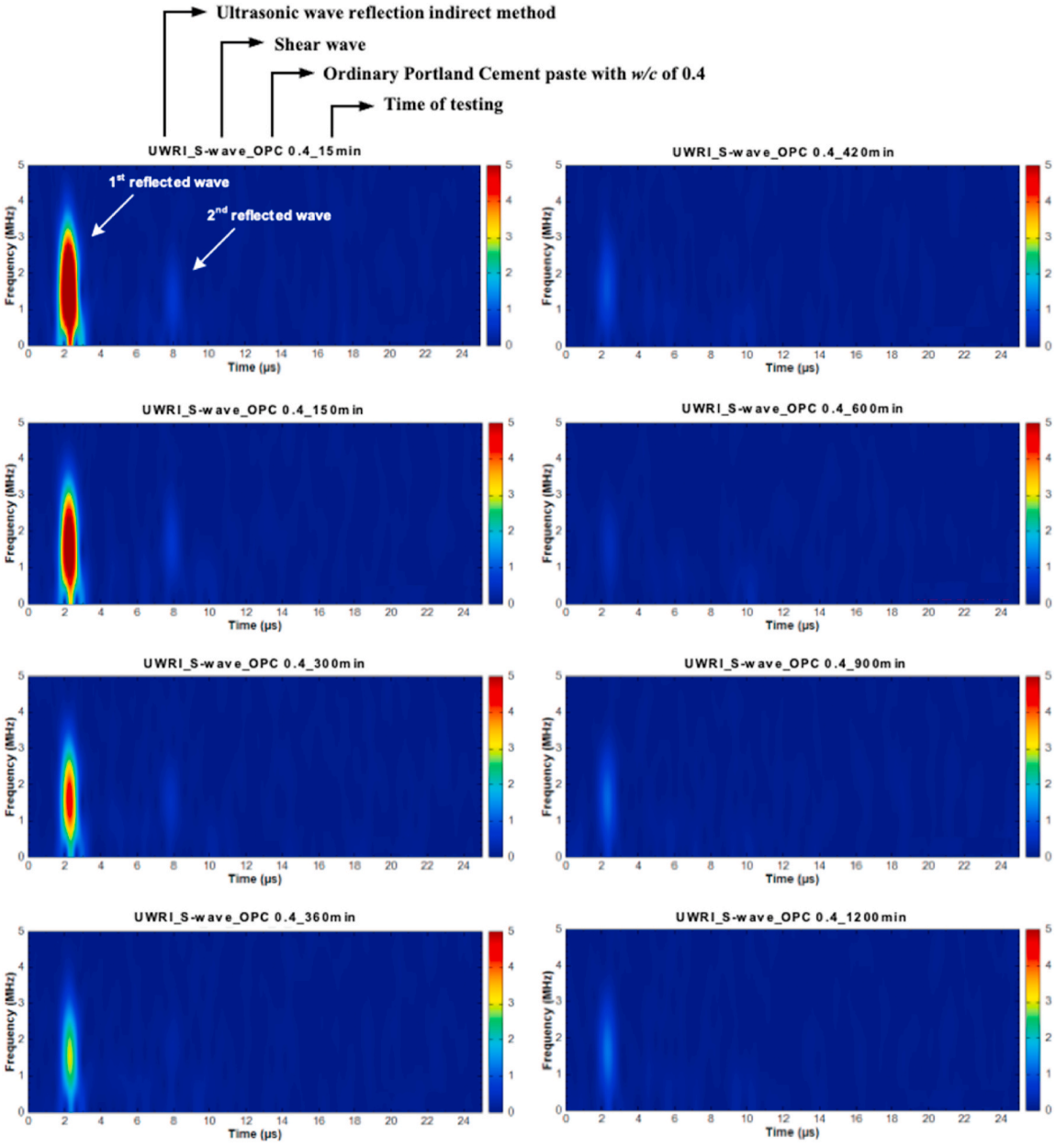

Fig. 8. Development of STFT waveform between 15 and 1200 min using the S-wave reflection at the acrylic–paste interface (UWRI method) (note: OPC 0.4 paste was taken as an example).

Moreover, as presented in Table 2, the UWRD method performed slightly better than UWRI because it eliminated the need for a buffer material. By reflecting waves directly within the paste, UWRD provided more reliable signals that better represent the paste's evolving structure, whereas UWRI's reflections may be weakened due to absorption or scattering at the buffer-paste interface. Additionally, UWRD reduced experimental uncertainty by eliminating inconsistencies in paste-buffer contact. These advantages make UWRD a more effective method for monitoring cement paste setting.

4.2. Analysis of ultrasonic wave reflection indirect method (UWRI) responses

In the UWRI method, the acrylic plate used as a buffer material plays an important role in analyzing the behavior of reflected waves as the paste transitioned from a liquid to a solid state using S-wave measurements. Since the elastic wave first interacts with the buffer material, the reflection responses differ significantly from those observed in the UWRD method. The typical reflection behavior at the acrylic plate-cement paste boundary was visualized using STFT transformation and is presented in Fig. 8 for the shear wave application.

According to Fig. 8, at the early stage (15 min), the signals were detected with having two reflected waves. The first reflected wave appeared at approximately at 2 μs, while the second reflected wave was located around 8 μs. As hydration progressed, the reflected wave amplitudes gradually decreased, leading to amplitude loss, as seen in the spectrum at 300 min. At a certain point, the first reflected wave reached its lowest amplitude, while the second reflected wave disappeared entirely. Beyond this time, the amplitude of the first reflected wave began to increase slightly and continued to do so up to 1200 min. This behavior was observed across all paste samples, though the disappearance of the reflected waves occurred at different times depending on the *w/c* of the paste. The specific time when the first reflected wave reached its minimum amplitude could be an important indicator of the setting time of cement paste. The evolution of wave reflection followed a distinct pattern: (i) at the beginning of the test, reflected waves were present; and (ii) suddenly, the reflected wave disappeared, followed by a slight increase in amplitude over time. Initially, the signal at the buffer-paste interface (after pouring the paste into the mould) remained stable compared to the initial signal at the buffer-air interface (before pouring the paste). This phenomenon confirmed that the shear wave could not penetrate a liquid-based medium. However, since the cement paste was a suspension of cement and water, it was not classified as a pure liquid. In the first few minutes after placing the paste in the mould, the amplitude of the reflected waves decreased gradually, confirming that the shear wave had begun to penetrate the paste. A typical FFT evolution over time is depicted in Fig. 9.

In general, the analysis of time-domain and frequency-domain signals using FFT followed a similar approach to that used in the UWRD method. However, unlike the UWRD method, normalization is required in the UWRI method because the FFT peak amplitudes in the spectra obtained from the ultrasonic tests may vary over time. To establish a reference, the boundary between the buffer material and air (before the paste was poured into the mould) was opted as the corresponding medium. The results obtained from reflections within the pastes were then normalized using the reflection at the air interface, as follows:

$$r(f) = \frac{F_1^{acrylic-paste}}{F_1^{acrylic-air}} \tag{6}$$

where $r(f)$ is normalized FFT peak amplitude, $F_1^{acrylic-paste}$ is magnitude of FFT at acrylic–paste interface, and $F_1^{acrylic-air}$ is magnitude of FFT at acrylic–air interface. The typical development of ultrasonic wave reflection response at the acrylic-cement paste interface is

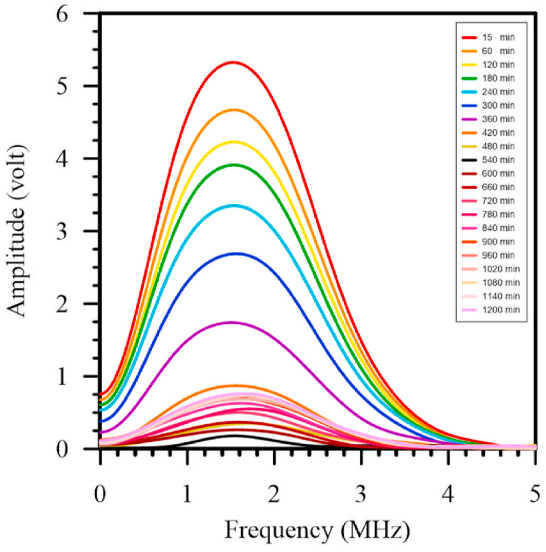

Fig. 9. A typical FFT evolution based on the S-wave UWRI measurement (note: OPC 0.4 paste was taken as an example).

presented in Fig. 10. The results showed that the degradation of FFT occurred as the paste hydrated over time, eventually reaching a minimum point, denoted as t_s, which represents the setting time. This stage signifies the continuous solid phase during very early hydration, while the development of cement particle percolation and entrapped pores as a complex network within the mixture is reflected in the decreasing rate of ultrasonic reflection [39]. When the solid volume fraction in cement paste mixtures increases, both the amplitude and reflection energy at the boundary decline, as the paste's impedance may approach that of the buffer [20]. The solid volume fraction plays a crucial role in the microstructural evolution of the cement paste, influencing hydration variations that, in turn, impact the stiffening process.

With higher *w/c*, the rate of solid structure formation due to hydration appears to be noticeably slower and more time is required to achieve the three-dimensional percolation associated with set [43]. Specifically at t_s, the FFT curve reached its lowest point before slightly increasing afterward. This point marks the initial slope change in the FFT curve, signifying the final setting time—the moment when the paste completely loses its plasticity. The t_s point also corresponds to the minimum FFT amplitude and the disappearance of the reflected wave spectrum in the STFT spectrogram. Beyond this point, a slight increase in FFT amplitude represents the hardening stage, during which the internal structure of the paste continues to develop. At this stage, hydration products create microstructural bridges within the percolated solid networks, and by increasing the elastic modulus, adequate connective strength is developed to withstand the external force from the free fall of the Vicat needle. After solid-phase percolation, continuous growth and formation of calcium hydroxide can lead to narrowing of the porosity pathway [39]. With time, calcium hydroxide is continuously generated to thicken the dense structures with C-S-H bridges. Therefore, sufficient contact strength and bonding within the solid skeleton are essential for effectively transmitting stress waves in early-age cement paste. Additionally, the good reproducibility of this method is demonstrated in Fig. 11, where three repeated tests on OPC 0.4 paste showed that t_s appeared at the identical time in each trial.

The comparison of ultrasonic response on normalized FFT peak amplitudes for all pastes is presented in Fig. 12. When comparing results from the UWRI method with the Vicat needle test, the lowest point in the FFT curves coincided with the final setting time of the cement paste. For the OPC 0.3 paste, the final setting time measured via Vicat needle test was 402 min, while the normalized FFT curve reached its minimum at 405 min with an amplitude of 0.481 V (or normalized amplitude of 0.076). The FFT amplitude then increased slightly until 800 min, after which it remained stable at an average amplitude of 1 V. Nevertheless, the FFT responses did not indicate a significant point for determining the initial setting time. Based on the Vicat result, the initial setting time was achieved when the normalized amplitude reached approximately 0.16. For the OPC 0.4 paste, the minimum point on the FFT curve appeared 31 min later than the final set time measured by the Vicat test. Conversely, for the OPC 0.5 paste, the t_s was recorded at 705 min, which was nearly identical to the Vicat test result at 706 min. Regarding the initial set time, it was observed that the initial setting time occurred when the normalized amplitudes reached approximately 0.1 and 0.075 for OPC 0.4 and OPC 0.5 pastes, respectively. This suggest that there is no definite relationship for determining the initial setting time based on FFT normalization. Table 2 summarizes the setting time results for all pastes, comparing the final set time obtained from the Vicat needle test with that determined using the UWRI S-wave reflection method. The results indicated that higher water content in the pastes delayed the minimum point of the FFT curve, as detected by ultrasonic testing. In addition, the development of paste's internal structure was more pronounced in mixtures with a lower *w/c* at an early age. From Table 2, the t_s from the UWRI method exhibited a strong correspondence with the t_f from the Vicat needle test. Ultimately, the UWRI method using shear wave can positively determine the final setting time of cement paste, with a difference of less than 6 % compared to the traditional Vicat needle measurement.

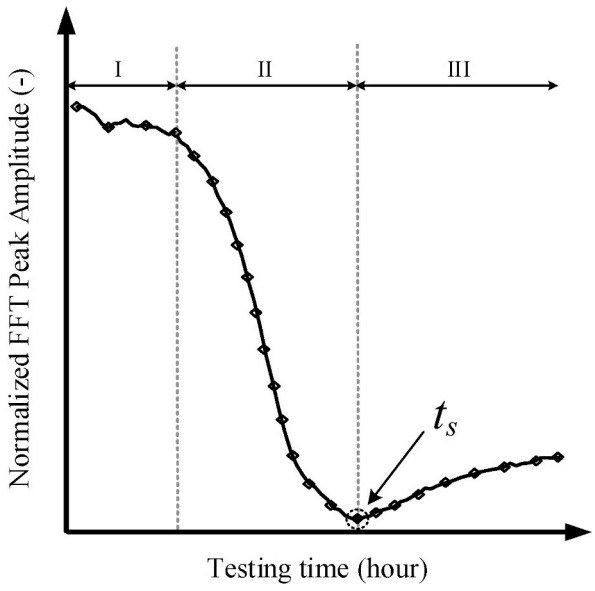

Fig. 10. A typical development of ultrasonic S-wave reflection response between the acrylic plate and cement paste via UWRI method.

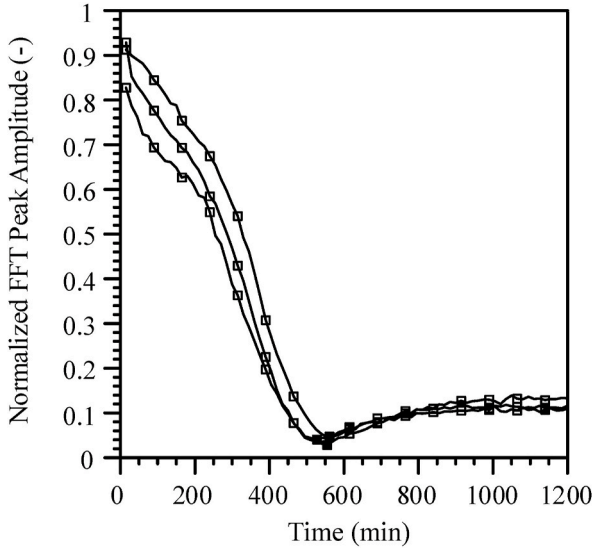

Fig. 11. Reproducibility of UWRI results with triplicates of OPC 0.4 pastes (note: points t_s were marked as filled square bullet).

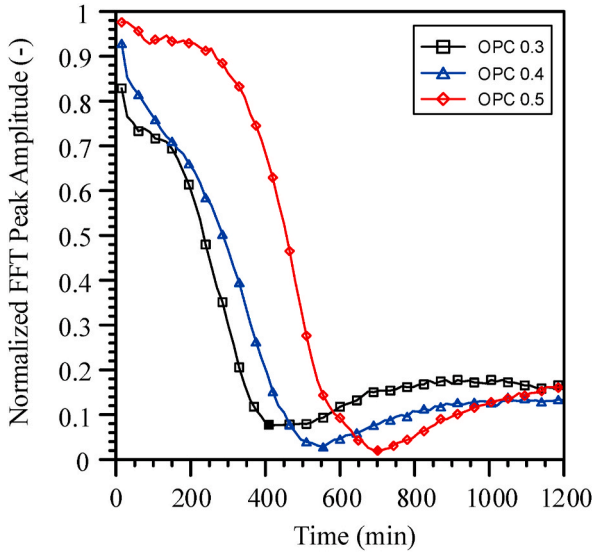

Fig. 12. Normalized FFT peak amplitudes on all cement pastes via S-wave reflection at the interface of acrylic–paste.

4.3. Comparison between hydration measurement and ultrasonic measurement

The hydration heat evolution of cement pastes with different *w/c* is shown in Fig. 13. A distinct thermal peak was observed in each paste at approximately 10–12h, corresponding to the hydration of silicate phases. The silicate hydration in the OPC fraction, which contributes to heat liberation in fresh pastes, was accelerated due to the dilution effect [44]. A higher *w/c* resulted in lower thermal peaks and a slight peak shift, indicating a prolonged hydration process. While the induction periods of all pastes appeared to be identical, the deceleration period was more pronounced in OPC 0.3 than in other pastes. This intensified deceleration phase may be linked to the higher formation of ettringite.

Moreover, the calorimetric results were compared with the ultrasonic results to analyze the occurrence of setting time, as depicted in Fig. 14. As a note, the UWRD results were normalized using the highest amplitude at 20 h, arranging the final value to 1 for consistency. Fig. 14 shows that the initial and final setting times occurred during the acceleration period, aligning with findings from previous studies [16,45,46]. However, no distinct points in the heat evolution curves could be identified to precisely determine the setting time. In contrast, the FFT analysis from ultrasonic measurements provided a clear indication of the final setting time, with the UWRD and UWRI results sharing similar values within a small margin. This confirms that there is no direct correlation between ultrasonic and calorimetric results to simultaneously define the setting time. Instead, both UWRD and UWRI methods demonstrate robust

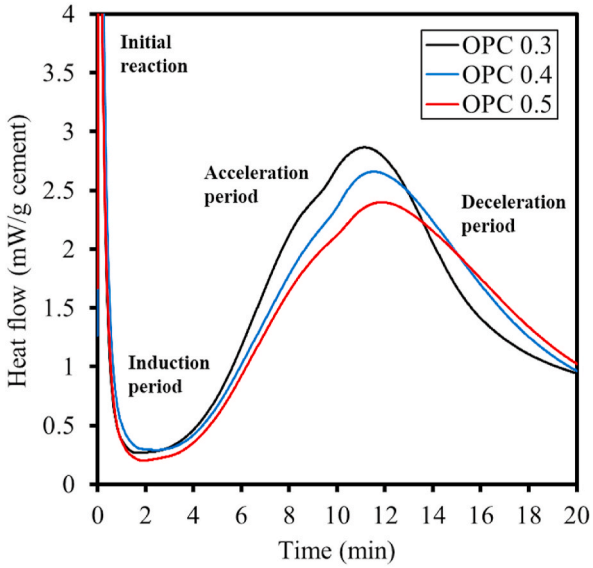

Fig. 13. Heat of hydration rate of cement pastes with different *w/c*.

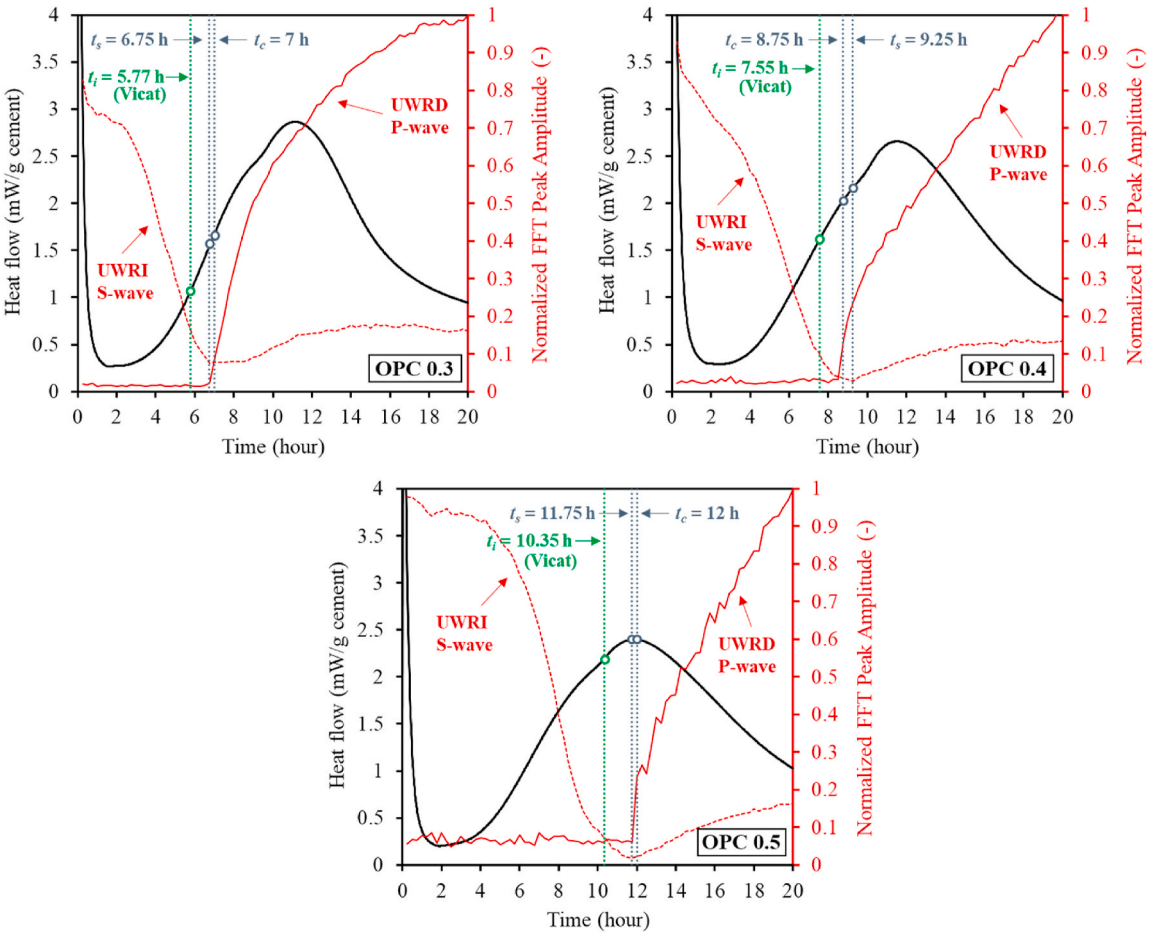

Fig. 14. Relationship between initial setting time (t_i from Vicat), final setting time (t_c from UWRD, t_s from UWRI) and heat of hydration rate.

accuracy in determining the final setting time of cement paste.

5. Discussion

5.1. Evolution of stiffening by ultrasonic reflection

To further emphasize the relationship between reflected wave appearance and the stiffening evolution of cement paste, the ultrasonic measurements results were categorized into several stages. According to the UWRD results, five stages were identified on the basis of typical curves as illustrated in Fig. 15.

In Stage I, before the paste is poured into the mould, the interface medium is air-to-air, meaning no reflection occurs at the boundary. Theoretically, when waves encounter two materials with identical acoustic impedance, they are fully transmitted without reflection. Since both the first and second mediums are air, all waves pass through without bouncing back. In Stage II, once the paste is poured into the mould, no significant reflected signal is detected, as the paste remains in a suspension state. Although P-waves can propagate through liquid, they require a distinct interface to reflect. At this stage, the energy loss is too high, preventing any reflected waves from returning to the transducer. Stage III marks the beginning of the stiffening process, corresponding to the initial setting time. However, reflected signals are still absent. As visualized in Fig. 15, the current paste consists of two layers: (i) the bottom layer behaves more like a solid (initial set depth = 25 mm), and (ii) the top layer remains semi-solid. Since the bottom layer is denser than the top, stiffening starts from the bottom and progresses upward. However, because the acoustic impedance of both layers is relatively similar, waves are fully transmitted with only partial energy loss, preventing detectable reflections. In Stage IV, the paste has completely solidified, reaching the final setting time. At this stage, the boundary condition shifts from a solid paste–semi-solid paste to a solid paste–air. Since the acoustic impedance difference between solid paste and air is now significant, waves reflect back to the transducer. However, the reflected wave energy remains low, as the paste has just solidified and has not yet developed considerable strength. In other words, the paste has not yet entered the hardening stage. Finally, in Stage V, the paste undergoes hardening, becoming solid and mature due to continued hydration. At this later age, reflected waves become stronger as the paste's strength and acoustic impedance increase progressively. The reflected signal in the time-domain waveform now correlates with the strength of the paste. Additionally, the influence of w/c on cement pastes aligns well with this stage-based reflection model, further validating the proposed concept.

The use of shear waves with a buffer material resulted in a different wave propagation behavior in cement paste in comparison with the UWRD method. Based on the UWRI results, the schematic representations of reflection behaviors at the acrylic-cement paste boundary are presented in Fig. 10, where three distinct stages can be identified. Stage I is defined as the dormant stage and in this stage, an initial slight drop in the reflection coefficient occurs, which is associated with the flocculation of cement particles [20]. During this stable period, the cement paste remains in a suspension state, leading to high attenuation and an absence of detectable reflected waves. Additionally, the rate of stiffening in the paste is low during this phase. Stage II is defined as setting stage and this stage is characterized by a clear decline in the FFT curve, indicating the progression of hydration and an increase in the acoustic impedance of cement paste. Both the initial and final setting times occur within this stage. The sharp drop in the FFT curve continues until it reaches its minimum point (t_s), marking the final setting time. The inversion of the FFT curve, where its slope changes, occurs when the paste becomes acoustically harder than the buffer material. As hydration progresses, the acoustic impedance of cement paste gradually surpasses that of the acrylic plate, indicating rapid stiffening until the paste fully solidifies. Finally, Stage III is defined as the hardening stage and at this stage, the FFT curve stabilizes, and the reflection response remains relatively unchanged. This phase represents the continued hardening of the paste as hydration further strengthens the internal structure. These stages have also been observed in previous studies [14,20,21], demonstrating consistency in describing the setting process, despite differences in measurement techniques and analysis methods.

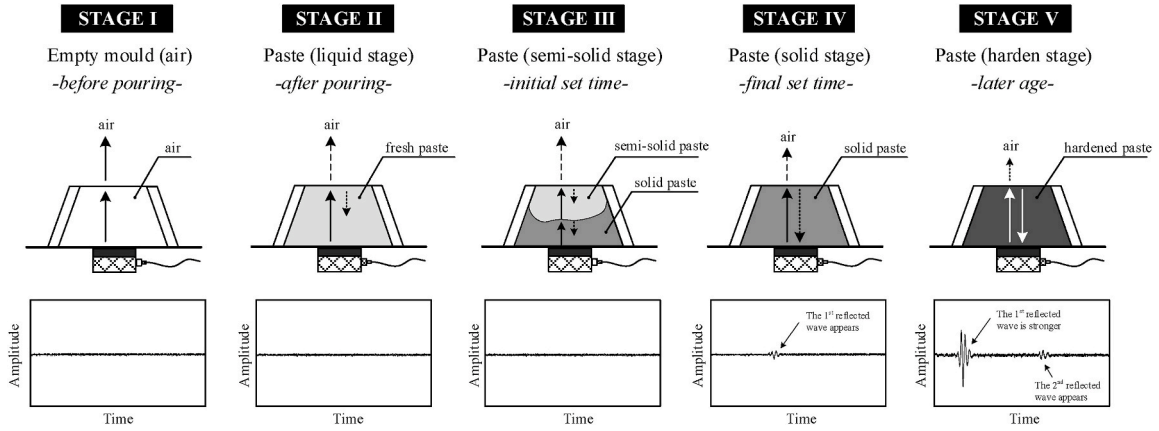

Fig. 15. Schematic representation of ultrasonic reflection response on the stiffening and hardening process of cement paste by the UWRD method.

5.2. Comparative studies on NDT techniques for setting time measurements

Table 3 compares the current study on UWRD and UWRI methods with the latest research on non-destructive testing (NDT) for measuring the setting time of cement-based materials. For instance, Park et al. [47] used a UTM apparatus to evaluate the setting time of cement paste and identified a specific point where velocity began to rise exponentially, corresponding to the initial setting time. The final setting time was determined by the peak of the first derivative of wave velocity. However, when compared to the Vicat test, UTM demonstrated greater accuracy in predicting the final setting time (99 %) than the initial setting time (70 %). The gradual increase in velocity during cement hydration made it difficult to precisely detect the initial setting time.

Misák et al. [48] investigated the correlation between velocity increments and temperature changes in the paste during the stiffening process. Although they identified certain points as potential setting time indicators, these points lacked accuracy and were not reproducible when tested with different materials. Similarly, Yim et al. [49] explored the feasibility of using both P-wave and S-wave to monitor the setting process of cement paste via UTM. Their results showed no distinct points in the evolution of P-wave velocity. However, when using the S-wave, they found that the birth time (or arrival time) of S-wave propagation coincided with the final setting time. This finding supports the results of the present study, where the arrival of the first reflected S-wave via UWRD also marks the final setting time – although the principles of both methods (UTM and UWRD) are fundamentally different. Nonetheless, as Yim et al. [49] emphasized, detecting the birth time highly depends on the equipment performance, including the resolution and power amplifier characteristics.

Xu et al. [50] improved the sensitivity of ultrasonic testing by developing and embedding a novel piezoelectric transducer inside the cement paste. While monitoring transmitted waves in the time-domain signal, they observed a sudden increase in P-wave amplitude by several orders of magnitude, which was closely associated with the final setting time. However, no distinct wave behavior was detected at the initial setting time.

Several novel NDT techniques have been tested for their feasibility in monitoring paste hydration. Hong et al. [51] proposed a contactless ultrasonic method in which a transducer positioned above the mortar sample generated incident waves that were then reflected as leaky Rayleigh waves at the boundary between air and fresh mortar. At the early stages of hydration, these waves could not be measured because of the lack of shear resistance. However, as hydration progressed and the mortar transitioned from a liquid to a solid state, leaky Rayleigh waves began propagating at the interface. The onset of these waves closely corresponded to the final setting time determined by the Vicat test. Nevertheless, this method was also unable to detect the initial setting time.

On the other hand, Xie et al. [52] developed a novel remote sensing method based on ground penetrating radar (GPR) to measure the moisture content of cement paste by tracking changes in its dielectric constant, allowing for the assessment of setting time. A key advantage of this technique is that the electromagnetic waves can penetrate multi-layered systems and reflected off interfaces with different impedances. Their results showed that the initial setting time was characterized by a rapid decrease in the dielectric constant, while the final setting time was marked by the peak of its derivative. The accuracy of this method reached more than 94 %, highlighting its robustness. Another sensor-based method was introduced by Yi et al. [53], who utilized a patch antenna sensor at the bottom of the paste. The sensing mechanism relied on changes in the dielectric constant of cement paste during hydration, which caused shifts in the resonant frequencies of the built-in antenna. Similar to the findings in Ref. [52], this technique allowed for moisture content evaluation. Both initial and final setting times were identified with high accuracy (over 94 %), with two distinct points observed: the initial setting time corresponded to the beginning of a rapid increase in the moisture content, while the final setting time coincided with the peak acceleration of moisture concrete.

Based on above advancements, it is evident that the ultrasonic transmission method (UTM) is generally preferred over the ultrasonic reflection method. One possible reason is its ease of use and straightforward interpretation. Unlike reflection-based techniques, UTM allows wave velocity to be analyzed directly in the time-domain signal without requiring advanced signal processing like FFT and STFT. Additionally, recent studies have eliminated the need for buffer materials, enabling direct signal transmission into cement paste [20,21]. Furthermore, S-waves are rarely used in ultrasonic applications compared to P-waves. This is because P-waves generate stronger signals with higher energy, leading to better detection and reduced signal attenuation. As reported by Ref. [49], S-waves are difficult to detect until the material has significantly stiffened. Nevertheless, both P- and S-waves can be utilized effectively as long as the robustness of NDT instrumentations is guaranteed. As shown in Table 3, even when using similar UTM approaches, different researchers employ different instrumentation, resulting in variations in test results. While some studies successfully predict both initial and final setting times based on distinct points in the waveform, others can only detect one. This discrepancy highlights the critical importance of instrument selection, including careful consideration of frequency bandwidth, amplifiers, oscilloscopes and power supply stability. Overall, most studies demonstrate a high accuracy in predicting the final setting time, as the increased material density at this stage allows ultrasonic waves to propagate and reflect with sufficient energy.

5.3. Scalability and integration of ultrasonic techniques into field applications

The UWRD and UWRI methods have shown great potential for accurately predicting the final setting time of cement paste, but their real-world applicability in construction sites may require adaptation to overcome operational challenges such as portability, ease of implementation and data interpretation. Traditional laboratory setups involve precisely controlled conditions, which are often difficult to replicate on-site. To make these methods viable for field applications, they must be integrated into portable and robust testing equipment that can withstand the surrounding field environment (e.g., temperature fluctuation, humidity, mechanical vibration) and uneven surfaces commonly found in construction environments. A major improvement would be the development of a handheld or automated ultrasonic testing device that incorporates ruggedized transducers, compact electronic components, and real-time data

Table 3
Latest research on the use of non-destructive testing for setting time measurement (note: accuracy = the results from NDT vs. Vicat needle test).

Reference	NDT method	Wave type	Buffer material	Signal detection for setting time		Accuracy (scale: 0–100 %)	Characteristic point in the waveform
				t_i	t_f		
Hermawan et al. (2025)	Ultrasonic Wave Reflection Direct (UWRD)	S-wave	–	–	✓	>95 %	The arrival of the first reflected wave (final)
	Ultrasonic Wave Reflection Indirect (UWRI)	P-wave	Acrylic	–	✓	>94 %	A minimum point in FFT curve, marking its slope change (final)
Xie et al. (2022) [52]	Ground penetrating radar (GPR) – reflection method	Electro-magnetic wave	Air	✓	✓	>94 %	+ The time when the dielectric constant begins to decrease rapidly (initial) + The maximum derivative of the dielectric constant (final)
Yi et al. (2021) [53]	Patch antenna sensor	–	–	✓	✓	>94 %	+ The time when the moisture content starts to increase rapidly (initial) + The maximum moisture content acceleration (final)
Hong et al. (2021) [51]	Contactless ultrasonic	R-wave	Air	–	✓	–	The initiation of leaky Rayleigh waves at an incident angle of 5° (final)
Xu et al. (2024) [50]	Ultrasonic transmission method (UTM) with the omnidirectional piezoelectric transducer	P-wave	–	–	✓	–	The order of magnitude in amplitude during cement hydration (final)
Uppalapati et al. (2021) [54]	UTM via Ultra Test	P-wave	–	✓	–	–	The end of the condensation stage of the ultrasonic velocity curves (initial)
Yim et al. (2016) [49]	Diffuse ultrasound (UTM)	P-wave	–	–	–	–	No distinct points observed
		S-wave	–	–	✓	–	The birth time of S-wave propagation (final)
Misák et al. (2020) [48]	Vikasonic method (UTM)	P-wave	–	✓	✓	>73 %	The intersection of tangent lines based on the velocity curve and temperature changes (initial and final)
Park et al. (2024) [47]	UTM	P-wave	–	✓	✓	70–99 %	+ An inflection point when the velocity started to rise exponentially (initial) + The peak derivative of the wave velocity (final)

processing software.

For the UWRD method, where ultrasonic waves are directly applied to the cement paste via a thin acrylic sheet, the challenge lies in ensuring consistent and stable contact between the transducer and the fresh cement surface. In a construction environment, this could be addressed by designing self-aligning or automated positioning mechanisms to minimize user dependency and improve reliability. A possible solution is the integration of a flexible mounting frame that holds the transducer in place, ensuring optimal wave transmission while adapting to surface irregularities. Alternatively, a non-contact variant using laser ultrasonics could be explored to eliminate the need for physical contact with the paste, making it more practical for large-scale concrete pours.

The UWRI method, which relies on reflection through a thicker buffer material, is inherently more suited for field use as it eliminates the need for direct sensor placement on fresh cement surfaces. This method could be adapted by incorporating pre-installed buffer plates in formwork or reusable mould, allowing continuous monitoring of the setting process without manual intervention. Construction sites could benefit from modular sensor systems embedded into formwork panels, enabling real-time monitoring of cement setting across multiple locations simultaneously.

Another critical factor in field adaptation is real-time data processing and automation. The analysis of ultrasonic signals using Fast Fourier Transform (FFT) evolution requires computational power that may not always be available on-site. To address this, an embedded data processing unit within the testing device could automatically interpret waveforms and provide instant feedback on setting time estimates. Additionally, integrating wireless connectivity (Bluetooth or IoT-based systems) would allow test results to be transmitted to mobile devices, tablets, or cloud-based construction management platforms, enabling site engineers to make immediate data-driven decisions. Automated alerts for initial and final setting times could improve workflow efficiency, reducing delays and optimizing resource allocation.

Beyond construction site implementation, the broader adoption of UWRD and UWRI methods has the potential to influence industry standards set by global organizations such as ASTM (American Society for Testing and Materials) and ISO (International Organization for Standardization). Current standard test methods (ASTM C191 [4] and ASTM C266 [5]), rely on mechanical penetration techniques, which are destructive, labor-intensive, and susceptible to operator variability. The introduction of non-destructive ultrasonic reflection techniques could lead to the development of new ASTM/ISO standards that define.

- Test protocols for ultrasonic-based setting time estimation, including procedural steps for UWRD and UWRI methods
- Standardized ultrasonic transducer specifications, ensuring repeatability across different cement types and mix designs
- Calibration guidelines for various environmental conditions, accounting for temperature, humidity, and cement composition variability
- Limiting criteria for ultrasonic signal changes, correlating velocity shifts or FFT patterns with setting time thresholds

If incorporated into ASTM and ISO standards, these methods could become the new industry benchmark for setting time evaluation, replacing traditional penetration-based techniques with faster, more precise, and fully automated solutions. The adoption of these standards could also influence regulatory policies enforced by organizations such as ACI (American Concrete Institute), Eurocode, and national construction authorities, requiring ultrasonic testing in critical infrastructure projects, where precise setting time estimation is crucial.

5.4. Potential environmental and economic benefits of the proposed methods

The UWRD and UWRI methods may offer environmental and economic advantages by improving efficiency, reducing material waste and enhancing sustainability in construction. One of the most promising environmental benefits is the reduction of cement overuse and material waste. Traditional methods, such as the Vicat needle test, require physical penetration of the sample, often leading to sample destruction and the need for additional materials. In contrast, the UWRD and UWRI methods are non-destructive, meaning they can be used repeatedly on the same sample or even directly in construction applications without generating excess waste. This translates to a lower demand for raw materials and a reduction in landfill waste, contributing to a more sustainable construction industry. By providing a more accurate, real-time assessment of setting, these ultrasonic methods allow for better control over mix proportions, curing conditions and material performance, preventing overuse of raw materials.

From an economic standpoint, the UWRD and UWRI methods may offer considerable cost savings by streamlining the construction process and improving quality control. The ability to monitor ultrasonic wave reflections allows for a detailed understanding of the hydration process, ensuring that cement paste reaches the required properties at the right time. This level of precision reduces reliance on trial-and-error methods, thereby minimizing errors, rework and material wastage, where all of which can be very costly in large-scale construction projects. Additionally, these ultrasonic techniques provide a more objective, automated, and reproducible approach compared to traditional manual testing, which can be subject to human error. As a result, the need for extensive labor and supervision is reduced, translating to lower labor costs and improved work efficiency.

Moreover, these methods enhance productivity by allowing for optimized construction scheduling. For instance, in large-scale projects such as bridges, high-rise buildings, and infrastructure developments, accurately predicting the final setting time ensures that formwork can be removed at the optimal moment, reducing downtime and expediting project timelines. Faster setting time assessments also contribute to safer and more reliable structures, as the risk of removing formwork too early (leading to structural failure) or too late (causing unnecessary delays) can be minimized.

The widespread adoption of UWRD and UWRI methods could have broader industry-wide economic impacts, particularly in regions with high construction demands. By standardizing ultrasonic reflection techniques for setting time estimation, governments and construction companies can establish more efficient regulatory frameworks, reducing the economic burden of quality control and compliance testing.

Conclusively, the UWRD and UWRI ultrasonic methods may provide a more efficient, cost-effective, and sustainable approach to monitoring the stiffening process. Their ability to reduce material waste, optimize cement usage, lower carbon emissions, improve construction scheduling, and minimize costs makes them a highly valuable advancement for both the construction industry and the environment. Their implementation has the potential to transform traditional cement testing methods, leading to greener and more economically viable building practices in the future.

6. Conclusions

This paper investigates the feasibility of ultrasonic wave reflection direct (UWRD) and indirect (UWRI) methods for monitoring the stiffening process of cement paste concerning its setting time. The UWRD method was developed and implemented using a thin layer of acrylic sheet to reflect the signal at the cement paste-air interface. In contrast, the UWRI method utilized an acrylic plate as a buffer material to reflect elastic waves at the acrylic-cement paste interface. Based on the extensive non-destructive tests, the following conclusions can be summarized as follows.

1. According to the UWRD method, the arrival of the first reflected wave exhibited the occurrence of the final setting time of Portland cement paste with the accuracy of more than 95 % as compared with that from the traditional Vicat setting time measurement. However, initial setting time could not be detected from any characteristic points in FFT results due to the signal remained in the noise spectrum.
2. The phenomenon of the direct reflection behavior on the cement paste via the UWRD method can be explained into five distinct stages: (i) no reflection on the medium of air-to-air, (ii) substantial energy loss resulting in noise spectrum when the paste was firstly introduced, (iii) the beginning of stiffening process without any observed reflected waves, (iv) the arrival of the first reflected wave, corroborating the final set time, and the boundary condition changed from paste-paste to paste-air, and lastly (v) the hardening stage where the paste became mature.

3. The final set time can also be determined by the UWRI method with considering the minimum point in the FFT curves via S-wave reflection, representing the initial change of FFT slope. In this method, the final set times had comparable results as the standardized final set times based on Vicat needle test with less than 6 % difference. The S-wave reflection behavior at the boundary of acrylic plate and cement paste can be distinguished into three stages: (i) dormant stage, (ii) setting stage and (iii) hardening stage.
4. The proposed techniques, based on the UWRD and UWRI methods, are effective for predicting the final setting time of cement paste, and the stiffening progress of cement paste can be monitored extensively via FFT and STFT.

Following this study, the ultrasonic reflection method, when combined with signal processing techniques, has proven effective in detecting the final setting time of cement paste. However, it is difficult to capture the initial setting time. Therefore, future research should explore the application of machine learning algorithms or the integration of embedded sensors within fresh paste to enhance ultrasonic monitoring during the initial phase. Additionally, this study focusses on Ordinary Portland Cement (OPC) as the main binder. Further investigation is needed to assess the applicability of the proposed methods to other cementitious materials and mixes incorporating chemical or mineral admixtures.

CRediT authorship contribution statement

Harry Hermawan: Writing – review & editing, Writing – original draft, Visualization, Validation, Supervision, Resources, Methodology, Investigation, Funding acquisition, Formal analysis, Data curation, Conceptualization. **Fariz Rifqi Zul Fahmi:** Writing – review & editing, Methodology, Conceptualization.

Declaration of competing interest

The authors declare that they have no known competing financial interests or personal relationships that could have appeared to influence the work reported in this paper.

Acknowledgement

The authors would like to acknowledge the lab support from National Taiwan University of Science and Technology to conduct this experimental study.

Data availability

Data will be made available on request.

References

[1] A.M. Neville, J.J. Brooks, Concrete Technology, Pearson Education Limited, Harlow, England, 2010.
[2] Q. Tran, J. Roesler, Contactless ultrasonic test system for set times of mortar and concrete, ACI Mater. J. 118 (2) (2021) 97–106, https://doi.org/10.14359/51729328.
[3] L. Lavagna, R. Nisticò, An Insight into the Chemistry of Cement—A Review, 13, MDPI, 2023, https://doi.org/10.3390/app13010203. Applied Sciences (Switzerland).
[4] ASTM C 191, Standard Test Method for Time of Setting of Hydraulic Cement by Vicat Needle, ASTM International, 2004.
[5] ASTM C 266, Standard Test Method for Time of Setting of Hydraulic-Cement Paste by Gillmore Needles [Internet], ASTM International, 2003.
[6] S.L.M. Ribeiro Filho, C. Thomas, L.M.P. Durão, A.L. Christoforo, C. Bowen, F. Scarpa, et al., Ultrasonic pulse velocity and physical properties of hybrid composites: a statistical approach, Hybrid Advances 2 (2023) 100024, https://doi.org/10.1016/j.hybadv.2023.100024.
[7] J. Lin, B. Tian, Z. Liang, E. Hu, Z. Liu, K. Wang, et al., Impact of water–cement ratio on concrete mechanical performance: insights into energy evolution and ultrasonic wave velocity, Materials 17 (15) (2024), https://doi.org/10.3390/ma17153651.
[8] R.D. Angelo, T.J. Plona, L.M. Schwartz, P. Coveney, Ultrasonic measurements on hydrating cement slurries onset of shear wave propagation, Adv. Cement Base Mater. 2 (1995) 8–14.
[9] G. Trtnik, M. Gams, Recent advances of ultrasonic testing of cement based materials at early ages, Ultrasonics 54 (2014) 66–75, https://doi.org/10.1016/j.ultras.2013.07.010.
[10] H. Mao, S. Lan, H. Mao, J. Ren, X. Yi, Z. Huang, et al., Experimental study on properties of ultrasonic coupling agent with graphene in NDT, Appl. Sci. 12 (3) (2022), https://doi.org/10.3390/app12031236.
[11] H. Guneyli, S. Karahan, A. Guneyli, N. Yapici, Water content and temperature effect on ultrasonic pulse velocity of concrete, Russ. J. Nondestruct. Test. 53 (2) (2017) 159–166, https://doi.org/10.1134/S1061830917020024.
[12] X. Zhang, K. Wei, J. Zuo, Y. Zhou, Y. Hu, Effects of admixtures on the mechanical characteristics and microstructure of coral aggregate mortar, J. Build. Eng. 60 (2022), https://doi.org/10.1016/j.jobe.2022.105182.
[13] E.N. Landis, S.P. Shah, Frequency-dependent stress wave attenuation in cement-based materials, J. Eng. Mech. 121 (June) (1995) 737–743.
[14] Y. Zhang, W. Zhang, W. She, L. Ma, W. Zhu, Ultrasound monitoring of setting and hardening process of ultra-high performance cementitious materials, NDT E Int. 47 (2012) 177–184, https://doi.org/10.1016/j.ndteint.2009.10.006.
[15] W. Zhang, Y. Zhang, L. Liu, G. Zhang, Z. Liu, Investigation of the influence of curing temperature and silica fume content on setting and hardening process of the blended cement paste by an improved ultrasonic apparatus, Constr. Build. Mater. 33 (2012) 32–40, https://doi.org/10.1016/j.conbuildmat.2012.01.011.
[16] E. John, B. Lothenbach, Cement hydration mechanisms through time – a review, Journal of Materials Science. Springer 58 (2023) 9805–9833, https://doi.org/10.1007/s10853-023-08651-9.
[17] W. Chen, Z. Shui, Y. Li, Early age hydration of cement paste monitored with ultrasonic velocity and numerical simulation, J. Wuhan Univ. Technol.-Materials Sci. Ed. 25 (4) (2010) 704–707, https://doi.org/10.1007/s11595-010-0075-2.
[18] T. Öztürk, O. Kroggel, P. Grübl, J.S. Popovics, Improved ultrasonic wave reflection technique to monitor the setting of cement-based materials, NDT E Int. 39 (4) (2006) 258–263, https://doi.org/10.1016/j.ndteint.2005.06.012.

[19] T. Öztürk, J. Rapoport, J.S. Popovics, S.P. Shah, Monitoring the setting and hardening of cement-based materials with ultrasound, Concrete Science and Engineering 1 (2) (1999) 83–91.
[20] C.W. Chung, P. Suraneni, J.S. Popovics, L.J. Struble, Using ultrasonic wave reflection to monitor false set of cement paste, Cem. Concr. Compos. 84 (2017) 10–18, https://doi.org/10.1016/j.cemconcomp.2017.08.010.
[21] C.W. Chung, P. Suraneni, J.S. Popovics, L.J. Struble, W.J. Weiss, Application of ultrasonic P-wave reflection to measure development of early-age cement-paste properties, Materials and Structures/Materiaux et Constructions 46 (6) (2013) 987–997, https://doi.org/10.1617/s11527-012-9948-5.
[22] G. Trtnik, M.I. Valič, G. Turk, Measurement of setting process of cement pastes using non-destructive ultrasonic shear wave reflection technique, NDT E Int. 56 (2013) 65–75, https://doi.org/10.1016/j.ndteint.2013.02.004.
[23] G. Trtnik, M.I. Valič, F. Kavčič, G. Turk, Comparison between two ultrasonic methods in their ability to monitor the setting process of cement pastes, Cement Concr. Res. 39 (10) (2009) 876–882, https://doi.org/10.1016/j.cemconres.2009.07.002.
[24] H.J. Yim, J.H. Kim, S.P. Shah, Ultrasonic monitoring of the setting of cement-based materials: frequency dependence, Constr. Build. Mater. 65 (2014) 518–525, https://doi.org/10.1016/j.conbuildmat.2014.04.128.
[25] Y. Akkaya, T. Voigt, K.V. Subramaniam, S.P. Shah, Nondestructive measurement of concrete strength gain by an ultrasonic wave reflection method, Materials and Structures/Materiaux et Constructions 36 (262) (2003) 507–514, https://doi.org/10.1617/13854.
[26] T. Voigt, T. Malonn, S.P. Shah, Green and early age compressive strength of extruded cement mortar monitored with compression tests and ultrasonic techniques, Cement Concr. Res. 36 (5) (2006) 858–867, https://doi.org/10.1016/j.cemconres.2005.09.005.
[27] T. Voigt, Z. Sun, S.P. Shah, Comparison of ultrasonic wave reflection method and maturity method in evaluating early-age compressive strength of mortar, Cem. Concr. Compos. 28 (4) (2006) 307–316, https://doi.org/10.1016/j.cemconcomp.2006.02.003.
[28] K.V. Subramaniam, J. Lee, B.J. Christensen, Monitoring the setting behavior of cementitious materials using one-sided ultrasonic measurements, Cement Concr. Res. 35 (5) (2005) 850–857, https://doi.org/10.1016/j.cemconres.2004.10.028.
[29] P. Suraneni, L.J. Struble, J.S. Popovics, C.-W. Chung, Set time measurements of self-compacting pastes and concretes using ultrasonic wave reflection, J. Mater. Civ. Eng. 27 (1) (2015) 1–8, https://doi.org/10.1061/(asce)mt.1943-5533.0001051.
[30] T. Voigt, G. Ye, Z. Sun, S.P. Shah, K. Van Breugel, Early age microstructure of Portland cement mortar investigated by ultrasonic shear waves and numerical simulation, Cement Concr. Res. 35 (5) (2005) 858–866, https://doi.org/10.1016/j.cemconres.2004.09.004.
[31] J.H. Kim, S.P. Shah, Z. Sun, H.-G. Kwak, Ultrasonic wave reflection and resonant frequency measurements for monitoring early-age concrete, J. Mater. Civ. Eng. 21 (9) (2009) 476–483, https://doi.org/10.1061/(asce)0899-1561(2009)21:9(476).
[32] Y. Nam, W. Kim, Y. Kim, T. Lee, S. Park, Analysis of influence of concrete aggregate in evaluation of form removal time of concrete using ultrasonic pulse velocity methods, J. Build. Eng. 86 (2024), https://doi.org/10.1016/j.jobe.2024.108775.
[33] Y. Xiao, Y. Miao, X. Zhang, Y. Xue, Gradient cement pastes with efficient energy dissipation and electromagnetic wave absorption, Commun. Eng. 4 (1) (2025), https://doi.org/10.1038/s44172-025-00375-9.
[34] N. Ospitia, R. Jaramani, O. Remy, D.G. Aggelis, Determination of concrete formwork removal time based on ultrasound reflection, Appl. Sci. 12 (3) (2022), https://doi.org/10.3390/app12031221.
[35] E.R. Fuller, A.V. Granato, J. Holder, E.R. Naimon, Ultrasonic studies of the properties of solids, Methods Exp. Phys. (1974) 371–441.
[36] K.F. Liu, H.K. Chai, N. Mehrabi, K. Yoshikazu, T. Shiotani, Condition assessment of PC tendon duct filling by elastic wave velocity mapping, Sci. World J. 2014 (2014), https://doi.org/10.1155/2014/194295.
[37] ASTM C 150, Standard Specification for Portland Cement [Internet], ASTM International, 2004.
[38] ASTM C 305, Standard Practice for Mechanical Mixing of Hydraulic Cement Pastes and Mortars of Plastic Consistency [Internet], ASTM International, 1999.
[39] H.J. Yim, Y.H. Bae, Y. Jun, Hydration and microstructural characterization of early-age cement paste with ultrasonic wave velocity and electrical resistivity measurements, Constr. Build. Mater. 303 (2021), https://doi.org/10.1016/j.conbuildmat.2021.124508.
[40] S. Basu, S. Sasmal, T. Kundu, Ultrasonic wave characteristics in multiscale cementitious materials at different stages of hydration, Ultrasonics 142 (2024), https://doi.org/10.1016/j.ultras.2024.107397.
[41] S. Popovics, Fundamentals of Portland cement concrete: a quantitative approach, in: Fresh Concrete, 1, John Wiley & Sons, Inc, New York, 1982.
[42] R.M. Kmack, K.E. Kurtis, L.J. Jacobs, J.Y. Kim, Assessment of air entrainment in fresh cement paste using ultrasonic nondestructive testing, ASTM (Am. Soc. Test. Mater.) Spec. Tech. Publ. 1511 STP (1) (2010) 1–26, https://doi.org/10.1520/stp49080s.
[43] P. Suraneni, J.S. Popovics, C.-W. Chung, L.J. Struble, Setting time measurement using ultrasonic wave reflection, ACI Mater. J. 109 (1) (2012).
[44] H.A. Nguyen, T.P. Chang, A. Thymotie, Enhancement of early engineering characteristics of modified slag cement paste with alkali silicate and sulfate, Constr. Build. Mater. 230 (2020) 117013, https://doi.org/10.1016/j.conbuildmat.2019.117013.
[45] L. Zheng, C. Xuehua, T. Mingshu, Hydration and setting time of MgO-type expansive cement, Cement Concr. Res. 22 (1) (1992) 1–5, https://doi.org/10.1016/0008-8846(92)90129-J.
[46] W. Zhang, F. Wu, Y. Zhang, Early hydration and setting process of fly ash-blended cement paste under different curing temperatures, J. Wuhan Univ. Technol.-Materials Sci. Ed. 35 (3) (2020) 551–560, https://doi.org/10.1007/s11595-020-2292-7.
[47] S. Park, J.H. Rhee, S. Baek, S. Pyo, G. Kim, A multi-frequency ultrasonic method for nondestructive detection of setting times and internal structure transition of building materials, Constr. Build. Mater. 425 (2024), https://doi.org/10.1016/j.conbuildmat.2024.136087.
[48] P. Misák, B. Kucharczyková, D. Kocáb, T. Vymazal, Ultrasonic NDT determination of initial and final setting time of cement paste, MATEC Web of Conferences 310 (2020) 00027, https://doi.org/10.1051/matecconf/202031000027.
[49] H.J. Yim, Y.K. An, J.H. Kim, Water depercolation of setting cement paste evaluated by diffuse ultrasound, Cem. Concr. Compos. 71 (2016) 10–19, https://doi.org/10.1016/j.cemconcomp.2016.04.003.
[50] D. Xu, N. Zhao, Y. Hu, S. Xu, huaicheng Chen, P. Liu, Ultrasonic monitoring of hydration behavior of cement paste doped with triethanolamine using novel piezoelectric ultrasonic transducer, Sens Actuators A Phys 366 (2024), https://doi.org/10.1016/j.sna.2024.115014.
[51] J. Hong, H. Choi, Monitoring hardening behavior of cementitious materials using contactless ultrasonic method, Sensors 21 (10) (2021), https://doi.org/10.3390/s21103421.
[52] L. Xie, Z. Xia, S. Xue, X. Fu, Detection of setting time during cement hydration using ground penetrating radar, J. Build. Eng. 60 (2022), https://doi.org/10.1016/j.jobe.2022.105166.
[53] Z. Yi, S. Xue, L. Xie, G. Wan, Detection of setting time in cement hydration using patch antenna sensor, Struct. Control Health Monit. 29 (2022).
[54] S. Uppalapati, L. Vandewalle, Ö. Cizer, Monitoring the setting process of alkali-activated slag-fly ash cements with ultrasonic P-wave velocity, Constr. Build. Mater. 271 (2021), https://doi.org/10.1016/j.conbuildmat.2020.121592.